EUROPEAN ORGANIZATION FOR NUCLEAR RESEARCH

L3 Note 2761
June 28, 2002

Measurements of the Cross Sections for Open Charm and Beauty Production in $\gamma\gamma$ Collisions at $\sqrt{s} = 189 - 209$ GeV

The L3 Collaboration

Abstract

The production of c and b quarks in $\gamma\gamma$ collisions is studied with the L3 detector at LEP with 627 pb^{-1} of data, collected at centre-of-mass energies from 189 GeV to 209 GeV. Hadronic final states containing c and b quarks are identified by detecting electrons or muons from their semileptonic decays. The cross sections $\sigma(e^+e^- \to e^+e^- c\bar{c}X)$ and $\sigma(e^+e^- \to e^+e^- b\bar{b}X)$ are measured and compared to next-to-leading order perturbative QCD calculations. The cross section of b production is in excess of the QCD prediction by a factor of three. The results presented in this Note are preliminary.

Submitted to the 31st *International Conference on High Energy Physics*
Amsterdam, Netherlands, 24-31 July 2002.

1 Introduction

The measurement of heavy flavour production in two-photon collisions provides a reliable test of perturbative QCD because of the large physical scale set by the charm or beauty quark mass. Many experiments have studied charm production in $\gamma\gamma$ collisions [1–3]. Beauty quark production in $\gamma\gamma$ collisions is expected to be suppressed by more than two orders of magnitude owing to its smaller electric charge and larger mass. At LEP energies, the direct and single resolved processes, shown in Figure 1, are predicted to give comparable contributions to the heavy flavour production cross section [4], whereas at low energies the direct process dominates. The main contribution to the resolved photon cross section is the photon-gluon fusion process $\gamma g \to c\bar{c}(b\bar{b})$. The production rate of c and b quarks in two-photon collisions therefore depends on their mass and the gluon density in the photon. Further contributions to charm production arise from the Vector Dominance Model (VDM) and from doubly resolved processes and are expected to be small.

This note describes the measurements of the inclusive open charm and beauty production performed with the L3 detector [5] with 627 pb^{-1} of data, collected at centre-of-mass energies from 189 GeV to 209 GeV. The note updates our previous measurement [3] which has been done with 410 pb^{-1} of data, collected at centre-of-mass energies from 189 GeV to 202 GeV.

We identify b and c quarks by tagging electrons [1)] or muons from their semileptonic decays. Due to the higher mass of the b quarks, these leptons are characterized by a higher momentum and higher transverse momentum than those from c quarks. The $b\bar{b}$ and $c\bar{c}$production cross section is measured here using the muon and electron transverse momentum spectra for both leptons having a momentum greater than 2 GeV. The charm cross section measurement is also made here by a simultaneous fit of transverse momentum spectra for charm and beauty fraction determination. Muons are always required to have a momentum greater than 2 GeV necessary to penetrate the calorimeters and reach the muon chambers, while electrons can be identified with momentum as low as 0.6 GeV [2].

2 Monte Carlo

The PYTHIA [6] Monte Carlo is used to model the two photon processes. The non-b events are generated with massless matrix elements [7] while for b events massive matrix elements are used. The resolved process uses the SaS1d photon structure function [8]. The two-photon luminosity function is implemented in the equivalent photon approximation (EPA) [9] with a cutoff $Q^2 < m_\rho^2$.

Background sources are $e^+e^- \to e^+e^-\tau^+\tau^-$, $e^+e^- \to Z/\gamma \to q\bar{q}$, $e^+e^- \to \tau^+\tau^-$ and $e^+e^- \to W^+W^-$. These processes are generated with JAMVG [10], PYTHIA, KORALZ [11] and KORALW [12] respectively. The detector simulation is performed using the GEANT [13] and GHEISHA [14] packages. The Monte Carlo events are reconstructed in the same way as the data. Time dependent detector inefficiencies, as monitored during the data taking period, are also simulated.

[1)] Electron stands for electron or positron throughout this paper.

3 Event Selection Procedure

The event selection is performed in two steps. The first one selects hadronic final states produced in two-photon collisions, the second identifies a c or b quark by its semileptonic decay.

3.1 Hadronic Two-Photon Events

Hadronic two-photon events are selected by requiring at least five tracks and a visible energy, $E_{\rm vis}$, below $\sqrt{s}/3$. The visible mass, $W_{\rm vis}$, of the event is calculated from the four-momentum vectors of the measured particles, tracks and calorimetric clusters including those from the small angle luminosity monitor. These particles are considered to be pions except for unmatched electromagnetic clusters considered as photons. $W_{\rm vis}$ has to be greater than 3 GeV. The cut on $E_{\rm vis}$ separates the two-photon process from annihilation processes, characterized by high visible energy. The background from $\rm e^+e^- \to e^+e^-\tau^+\tau^-$ and $\rm e^+e^- \to \tau^+\tau^-$ events is suppressed by the requirement on the number of tracks.

The analysis is limited to untagged events with small photon virtuality. Events are excluded when the most energetic cluster in the small angle calorimeters has an energy greater than 0.2 $\sqrt{\rm s}$. Thus the interacting photons are quasi-real: $\langle \rm Q^2 \rangle \cong 0.015$ GeV^2, where $-\rm Q^2$ is the mass squared of the virtual photon.

3.2 Lepton Selection

Electrons from charm and beauty semileptonic decays are identified by requiring electromagnetic clusters in the polar angle range $|\cos\,\theta| < 0.725$ with momentum greater than 0.6 GeV. They should satisfy the following criteria:

- The candidate cluster is required to match to a track. The difference between the azimuthal angle between the shower barycentre and the track impact point at the calorimeter must be less than 20 mrad.
- The distribution of energies measured in the crystals of the calorimeter should be compatible with that of an electromagnetic cluster.
- The $\rm E_t/p_t$ ratio must be equal to one within 2σ, where $\rm E_t$ is the projection of the energy of the cluster on the plane transverse to the beam, $\rm p_t$ is the transverse momentum of the track and σ is the resolution on this ratio.
- Photon conversions are suppressed by requiring the distance of closest approach of the track to the mean $\rm e^+e^-$ collision point in the transverse plane to be less than 0.5 mm and the invariant mass of the electron candidate and of the closest track to be greater than 0.1 GeV.

After these cuts, 3850 events remain. The background from annihilation processes and two-photon production of tau pairs is estimated to be 0.75%.

Muon candidates are selected from tracks in the muon chambers in the angular range $|\cos\,\theta| < 0.8$. The momentum of the muons must be greater than 2.0 GeV. To suppress background from annihilation processes, the muon momentum must be less than 0.1 $\sqrt{\rm s}$. After all cuts are applied, 435 events remain. The estimated background from annihilation processes and two-photon production of tau pairs is 6.0%.

4 Total cross section $\sigma(e^+e^- \to e^+e^-b\bar{b}X)$

The b cross section is derived from a fit to the data distributions for events where the momentum of the muon or electron candidate is greater than 2.0 GeV, corresponding to 435 and 219 events respectively. The b selection efficiency is 2.20% for muons and 1.25% for electrons. The transverse momentum of the lepton with respect to the nearest jet, P_t, is chosen as the fit variable since it has the highest sensitivity to the b fraction. The jets are reconstructed using the JADE algorithm [15] with $y_{cut} = 0.1$. The energy of the muon or electron is not included in the jet.

A χ^2 fit is performed to the data distributions using the sum of the Monte Carlo distributions of the non two-photon background N_{bkg}, light quark events N_{uds}, c quark events $N_{c\bar{c}}$ and b quark events $N_{b\bar{b}}$. A three parameter fit is applied in which the number of beauty, charm and light quarks are free parameters, whereas N_{bkg} is held fixed according to the Monte Carlo prediction. The results of the fit are given in Table 1 which shows also the charm cross section estimate from the fit of the muon and electron P_t spectra.

The fit for muons yields a b fraction of 41.2 ± 3.8 (stat) %. As for the electrons, the b fraction is 46.2 ± 5.1 (stat) %. The χ^2 per degree of freedom for the muon and electron fits are 6.4/6 and 13.7/6 respectively. obtained for muon and electron respectively. The signal events are produced in two separate samples for direct and resolved processes assuming a 1:1 ratio [4]. The fitted distributions are shown in Figures 2 and 3.

The resulting cross sections for the luminosity averaged centre-of-mass energy $\langle\sqrt{s}\rangle = 198$ GeV are:

$$\sigma(e^+e^- \to e^+e^-b\bar{b}X)_{\text{muons}} = 13.0 \pm 2.35 \text{ (stat)} \pm 2.3 \text{ (syst) pb}$$

$$\sigma(e^+e^- \to e^+e^-b\bar{b}X)_{\text{electrons}} = 12.6 \pm 2.4 \text{ (stat)} \pm 2.3 \text{ (syst) pb.}$$

The systematic uncertainties arise from the event selection, jet reconstruction, massive or massless charm quarks in the event generation, b semileptonic branching ratio, trigger efficiency, Monte Carlo statistics and direct to resolved process ratio. Table 2 shows the values of systematic uncertainties due to these contributions. The dominant uncertainty comes from the event selection. It is estimated by variation of the cuts and includes detector resolution uncertainties and the agreement between data and Monte Carlo. The systematic uncertainty on jet reconstruction is assigned by variation of the y_{cut} parameter. The contribution due to the uncertainty on the ratio of the direct to the resolved processes is estimated by changing it from 1:1 to 1:2 or 2:1.

The muon and electron tag results are consistent. The combination of muon and electron results gives

$$\sigma(e^+e^- \to e^+e^-b\bar{b}X)_{\text{combined}} = 12.8 \pm 1.7 \text{ (stat)} \pm 2.3 \text{ (syst) pb.}$$

The result is in agreement with our previous measurement [3] and has an improved precision. The results are preliminary.

5 Total cross section $\sigma(e^+e^- \to e^+e^-c\bar{c}X)$

In the reference [3] the charm cross section has been measured with high statistical accuracy using the electron sample with momentum cut relaxed from 2 GeV to 0.6 GeV. In this note we did not perform again that analysis but rather the estimation of charm production is derived

by a simultaneous fit to the b and c fractions described in the previous section. The fit results are reported in Table 1. The resulting cross sections for the luminosity averaged centre-of-mass energy $\langle\sqrt{s}\rangle = 198$ GeV are:

$$\sigma(\mathrm{e^+e^-} \to \mathrm{e^+e^-c\bar{c}X})_{\mathrm{muons}} = 980. \pm 157.\ (\mathrm{stat})\ \mathrm{pb}$$

$$\sigma(\mathrm{e^+e^-} \to \mathrm{e^+e^-c\bar{c}X})_{\mathrm{electrons}} = 1039. \pm 180.\ (\mathrm{stat})\ \mathrm{pb}.$$

The combination of muon and electron results gives

$$\sigma(\mathrm{e^+e^-} \to \mathrm{e^+e^-c\bar{c}X})_{\mathrm{combined}} = 998. \pm 117.\ (\mathrm{stat})\ \mathrm{pb}.$$

This is in good agreement with the measurement of reference [3].

6 Comparisons with QCD Predictions

The cross sections for open beauty and charm production are compared in Figure 4 to perturbative next-to-leading order QCD calculations [4]. The dashed line corresponds to the direct process, NLO QCD calculations, while the solid line shows the prediction for the sum of direct and resolved processes. The direct process depends upon the QCD coupling constant and the heavy-quark mass. The prediction for open charm is calculated using a charm mass of either 1.3 GeV or 1.7 GeV and the open charm threshold energy is set to 3.8 GeV. The theory prediction for the resolved process is calculated with the GRV parton density function [17]. The renormalization and factorization scales are chosen to be the heavy quark mass. The direct process $\gamma\gamma \to \mathrm{c\bar{c}}$ is insufficient to describe the data, even if real and virtual gluon corrections are included. The data therefore require a significant gluon content in the photon.

The prediction for open beauty is calculated for a b quark mass of 4.5 GeV or 5.0 GeV and the open beauty threshold energy is set to 10.6 GeV. For $\langle\sqrt{s}\rangle = 194$ GeV and a b quark mass of 4.5 GeV, this cross section is 4.4 pb. The $\mathrm{b\bar{b}}$ cross section is measured in $\gamma\gamma$ collisions for the first time and is a factor of 3 and about 5 statistical uncertainty standard deviations higher than expected.

References

[1] JADE Collab., W. Bartel *et al.,* Phys. Lett. **B 184** (1987) 288,
TPC/Two-Gamma Collab., M. Alston-Garnjost *et al.,* Phys. Lett. **B 252** (1990) 499.
TASSO Collab., W. Braunschweig *et al.,* Z. Phys. **C 47** (1990) 499.
TOPAZ Collab., R. Enomoto *et al.,* Phys. Lett. **B 328** (1994) 535; Phys. Rev. **D 50** (1994) 1879; Phys. Lett. **B 341** (1994) 99; Phys. Lett. **B 341** (1994) 238.
VENUS Collab., S. Uehara *et al.,* Z. Phys. **C 63** (1994) 213.
AMY Collab., T. Aso *et al.,* Phys. Lett. **B 363** (1995) 249; Phys. Lett. **B 381** (1996) 372.
ALEPH Collab., D. Buskulic *et al.,* Phys. Lett. **B 355** (1995) 595;
L3 Collab., M. Acciarri *et al.*, Phys. Lett. **B 467** (1999) 137.

[2] L3 Collab., M. Acciarri *et al.*, Phys. Lett. **B 453** (1999) 83; Phys. Lett. **B 514** (2001) 19; Phys. Lett. **B 536** (2002) 217.

[3] L3 Collab., M. Acciarri *et al.*, Phys. Lett. **B 503** (2001) 10.

[4] M. Drees *et al.*, Phys. Lett. **B 306** (1993) 371.

[5] L3 Collab., B. Adeva *et al.*, Nucl. Instr. Meth. **A 289** (1990) 35;
M. Acciarri *et al.*, Nucl. Instr. Meth. **A 351** (1994) 300;
M. Chemarin *et al.*, Nucl. Instr. Meth. **A 349** (1994) 345;
I.C. Brock *et al.*, Nucl. Instr. Meth. **A 381** (1996) 236;
A. Adam *et al.*, Nucl. Instr. Meth. **A 383** (1996) 342.

[6] PYTHIA version 5.722 is used.
T. Sjöstrand, Preprint CERN-TH/7112/93 (1993), revised August 1995; Comp. Phys. Comm. **82** (1994) 74.

[7] M. Cacciari *et al.,* Nucl. Phys. **B 466** (1996) 173.

[8] G.A. Schuler and T. Sjöstrand, Z. Phys. **C 68** (1995) 607; Phys. Lett. **B 376** (1996) 193.

[9] V.M. Budnev *et al.,* Phys. Rep. **15** (1975) 181.

[10] J.A.M. Vermaseren, Nucl. Phys. **B 229** (1983) 347.

[11] KORALZ version 4.02 is used.
S. Jadach, B.F.L. Ward and Z. Wąs, Comp. Phys. Comm. **79** (1994) 503.

[12] KORALW version 1.33 is used.
S. Jadach *et al.,* Comp. Phys. Comm. **94** (1996) 216;
S. Jadach *et al.,* Phys. Lett. **B 372** (1996) 289.

[13] GEANT version 3.15 is used.
R. Brun *et al.*, Preprint CERN DD/EE/84-1 (1984), revised 1987.

[14] H. Fesefeldt, RWTH Aachen Report PITHA 85/2 (1985).

[15] JADE Collab., W. Bartel *et al.,* Z. Phys. **C 33** (1986) 23;
JADE Collab., S. Bethke *et al.,* Phys. Lett. **B 213** (1988) 235.

[16] ALEPH, DELPHI, L3 and OPAL Collab., Nucl. Instr. Meth. **A 378** (1996) 101.

[17] M. Glück, E. Reya and A. Vogt, Phys. Rev. **D 46** (1992) 1973.

Fit results	Muon Tag	Electron Tag
N_{bkg}	24.8 (fixed)	4.4 (fixed)
$N_{b\bar{b}}$	172.0 ± 31.0	94.3 ± 18.3
$N_{c\bar{c}}$	220.5 ± 35.4	105.4 ± 17.9
N_{uds}	$0.0^{+52.3}_{-\ 0.0}$	$0.0^{+12.0}_{-0.0}$
χ^2 / d.o.f.	6.4 / 6	13.7 / 6
$\sigma(e^+e^- \to e^+e^-b\bar{b}X)$, (pb)	13.0 ± 2.35	12.6 ± 2.4
$\sigma(e^+e^- \to e^+e^-c\bar{c}X)$, (pb)	980 ± 157	1039 ± 180

Table 1: Fit to the distribution of the transverse momentum of the lepton with respect to the nearest jet. The fit parameters are constrained to be positive. The correlation between $N_{b\bar{b}}$ and $N_{c\bar{c}}$ is 75%.

Source of uncertainty	Muon Tag	Electron Tag
	$\Delta\sigma(e^+e^- \to e^+e^-b\bar{b}X)$, %	$\Delta\sigma(e^+e^- \to e^+e^-b\bar{b}X)$, %
Event selection	14.6	15.8
Jet reconstruction	8.2	8.2
Massive/massless charm	3.0	3.0
$B(b \to e, \mu)$	2.0	2.0
Trigger efficiency	2.0	2.0
Monte Carlo statistics	1.4	1.8
Direct / resolved ratio	1.0	0.9
Total	17.3	18.4

Table 2: Systematic uncertainties on $\sigma(e^+e^- \to e^+e^-b\bar{b}X)$.

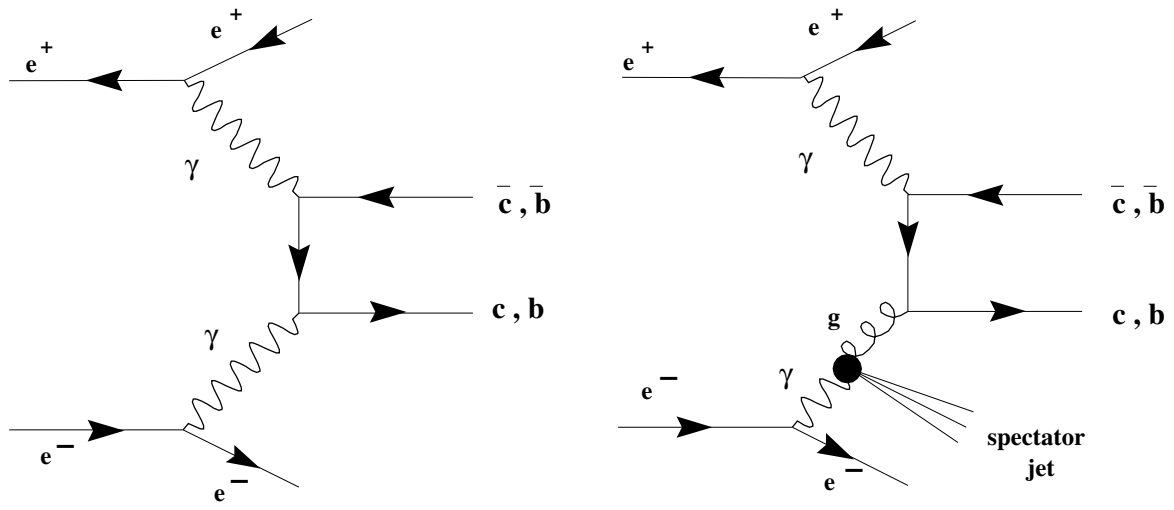

Figure 1: Diagrams contributing to charm and beauty production in $\gamma\gamma$ collisions at LEP.

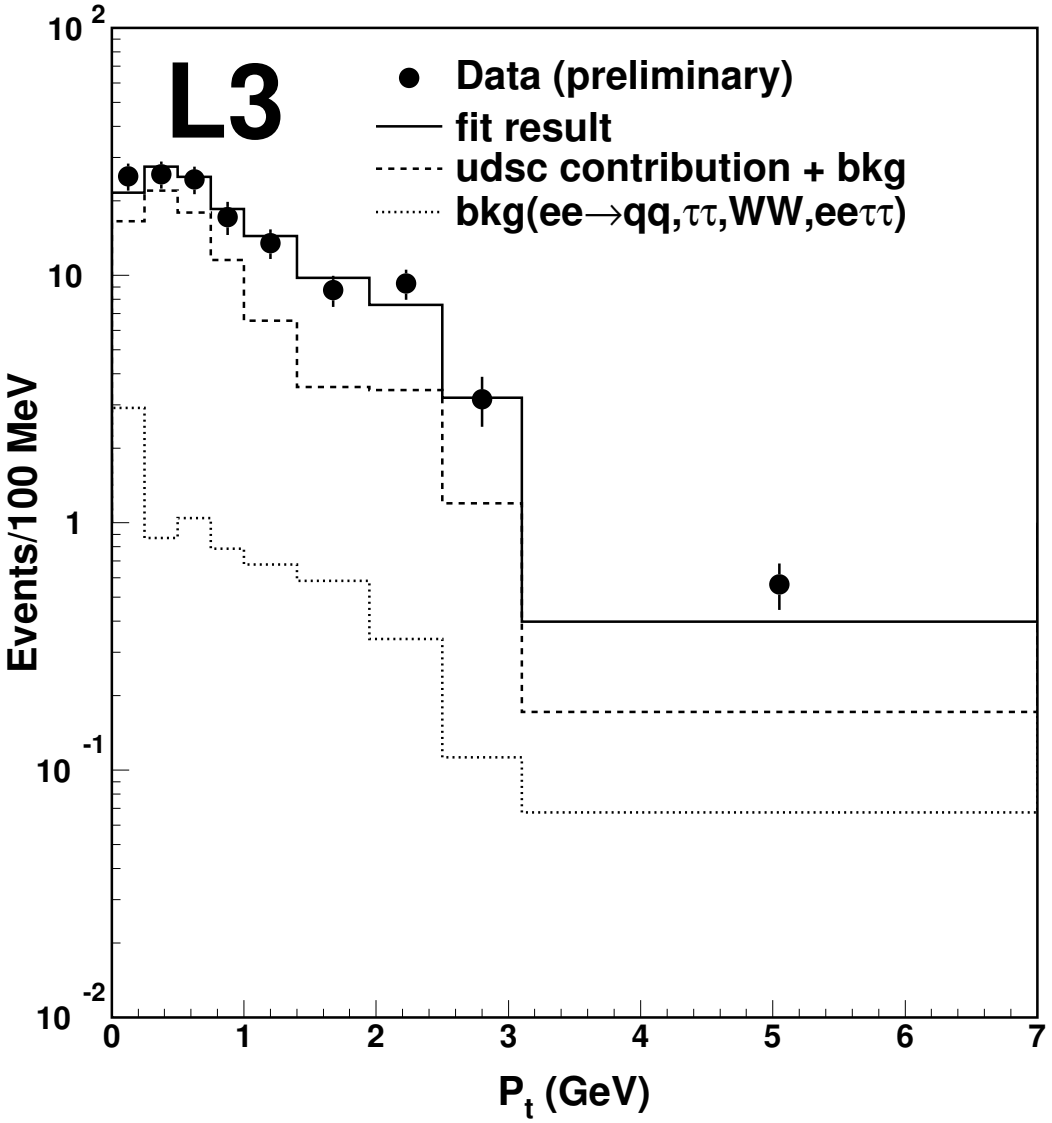

Figure 2: The distribution of the transverse momentum, P_t, of the muon candidate with respect to the closest jet.

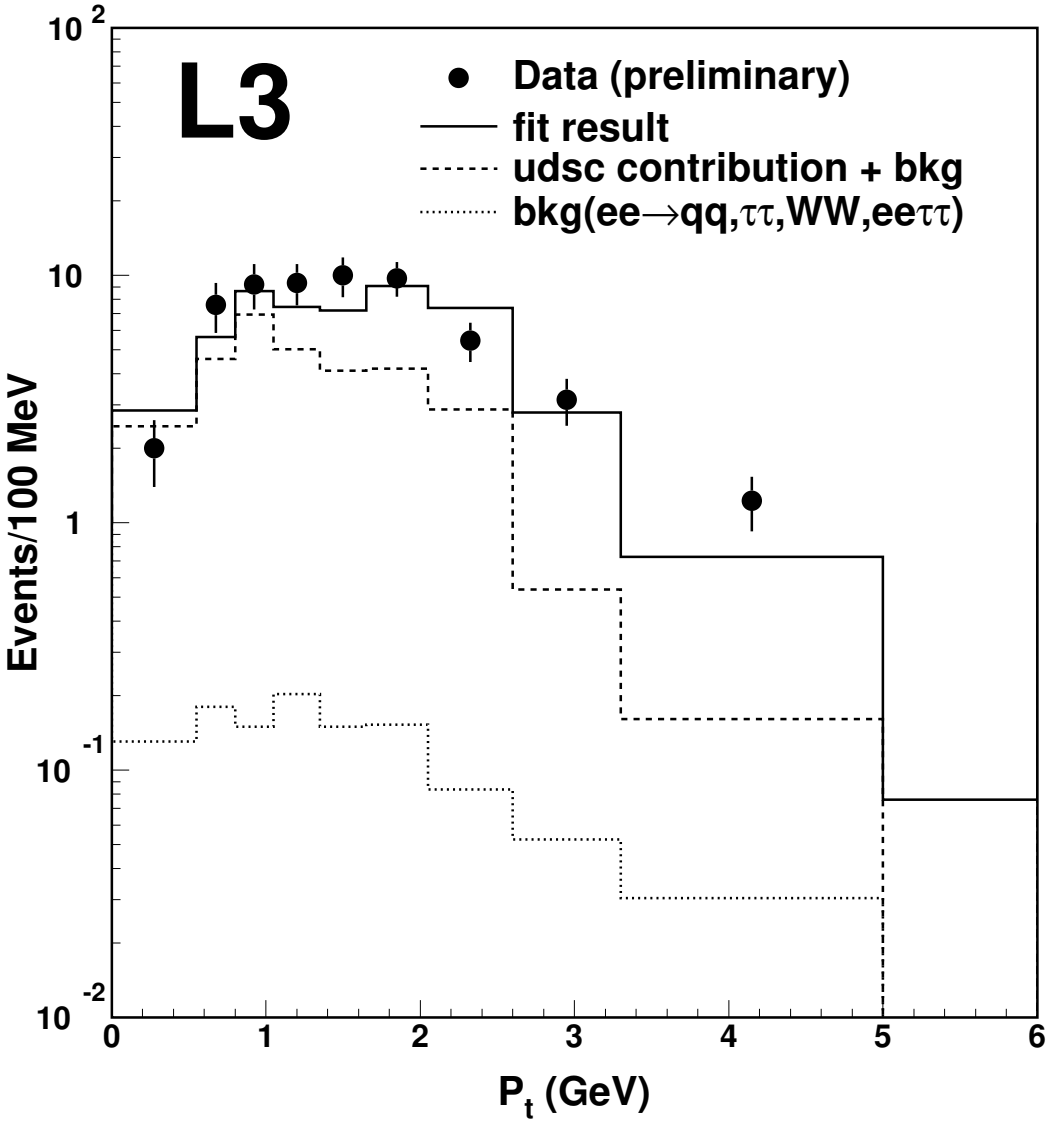

Figure 3: The distribution of the transverse momentum, P_t, of the electron candidate with respect to the closest jet.

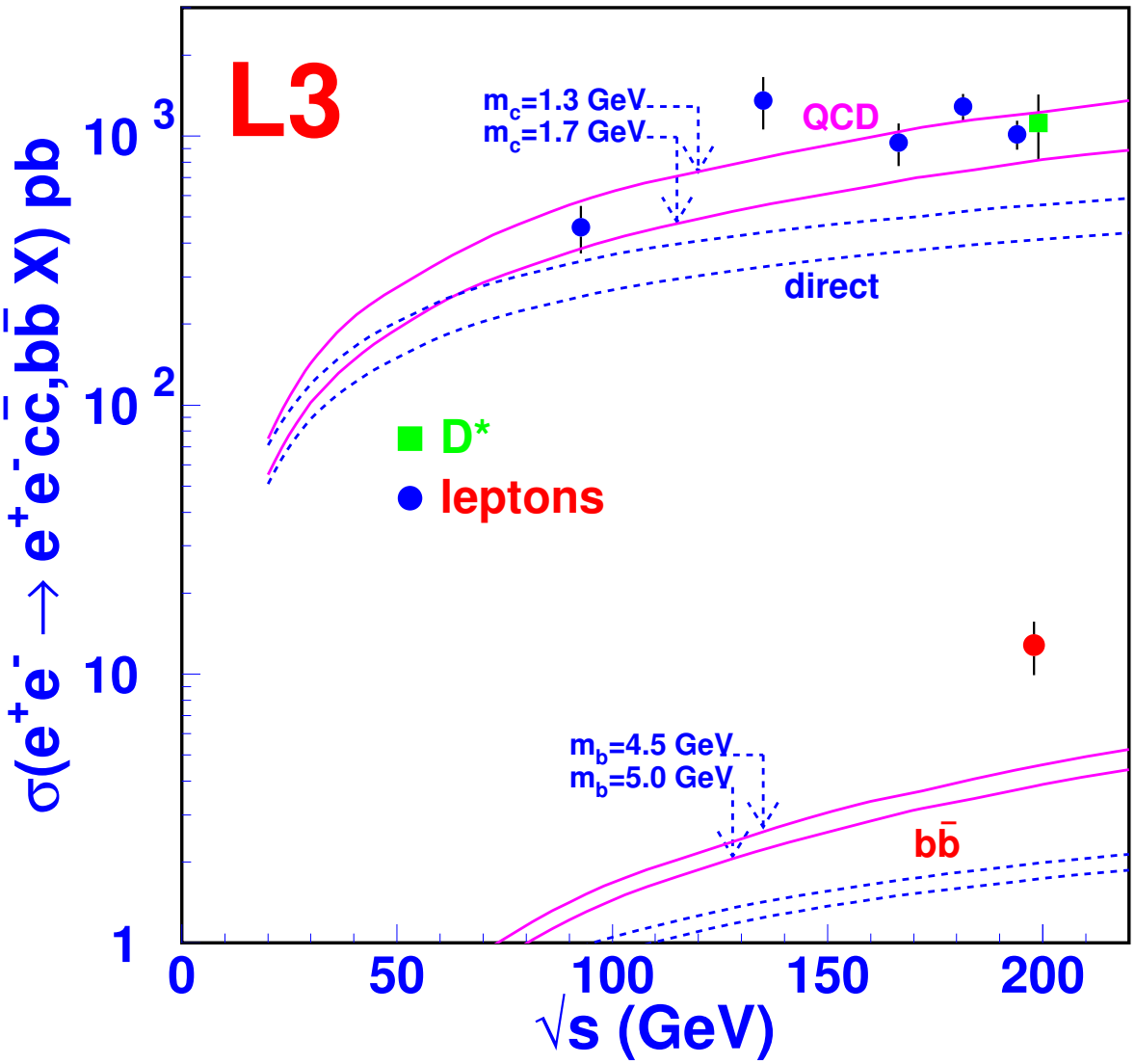

Figure 4: The open charm and beauty production cross section in two-photon collisions. The L3 data from both electron and muon events are combined. The statistical and systematic uncertainties are added in quadrature. The dashed line corresponds to the direct process contribution and the solid line represents the NLO QCD prediction for the sum of the direct and resolved processes.